

Effects of Poisson's ratio on the deformation of thin membrane structures under indentation

Jensen Aw^{*1}, Hongyi Zhao¹, Andrew Norbury¹, Lisa Li, Glynn Rothwell¹ and James Ren¹

¹ School of Engineering, Liverpool John Moores University, Byrom Street, Liverpool L3 3AF, UK.

Keywords indentation, bending, membrane, auxeticity.

Deformation/deflection of thin shells/membranes with clamped boundaries is a common material behaviour relevant to many engineering and medical conditions. A detailed understanding of the deformation mechanisms of different materials/structures with different Poisson's ratios under such a loading condition is of great significance to materials testing and product development. In this work, the deformation of circular elastic membranes with a clamped edge under point loading and finite contact conditions is systematically studied incorporating auxeticity behaviours. The effect of Poisson's ratio on the deformation of the material is investigated and the influence of parameters including sample thickness, indentation depth

and indenter size is analysed. The feasibility and limitation of an analytical solution is evaluated. The work shows that the P/δ^3 relationship is applicable to describe the force displacement data over the membrane domain for both point loading and finite contact conditions. It is shown that negative Poisson's ratios have direct influence on the membrane deformation domain, including the force-displacement curve, the deflection profile and the contact area. Critical factors affecting the P-h curves and the deformation mechanisms are discussed with reference to potential use of the Poisson's ratio effects.

Copyright line will be provided by the publisher

1 Introduction Many engineering and medical conditions involve deformation/deflection of thin shells/membranes with a clamped boundary, such as pressure sensors, valves and actuators as well as biological tissues [1-5]. The material deformation in these cases covers a wide spectrum of strain levels from small deformation to large displacement with samples of different thicknesses. A typical way to test the material behaviour is by using indentation bending tests in which an indenter/sphere is pressed onto a thin sample fixed along its rim of either a regular (round, square) or arbitrary shape [1,5]. The resulting force displacement curve (P-h curves) is dependent on the properties of the material, the structure and dimensions of the sample. A detailed understanding of the deformation mechanism of different materials/structures under such a loading condition is of great significance to materials testing and product development. Many studies have been conducted into the mechanics of membranes under localised load with different loading or boundary conditions [1-4, 6-9]. For example, in the work by Ju et al [1], a linear elastic solution is used to quantitatively interpret the measured central deflection of the membrane

under a circular concentrated load with an atomic force microscope. Experimental and theoretical investigations have also been conducted on problems of puncturing a membrane by a rigid cylinder [10]. Scott et al [3] compared the deformation of thin silicon and unfilled PDMS-based films loaded with different sized indenters over different strain regimes. Most of these works have been focused on material stiffness (represented by the Young's modulus) with a fixed Poisson's ratio. With the rapid development in materials with different Poisson's ratios, including material with negative Poisson's ratios at different length scales [11-18], it is important to investigate the potential effects of Poisson's ratio and auxeticity on the force-displacement data, the material deformation modes and its interaction with the indenter.

Due to the nature of loading and sample configuration, the effect of Poisson's ratio for sample with clamped edge conditions is complicated, being affected by material properties as well as the experimental conditions (such as sample thickness and indenter size, etc.). Within the loading domain, the deformation mode may change with depth. In the bending/plate domain, the load is known to be not affected by the

* Corresponding author: e-mail C.S.Aw@2010.ljmu.ac.uk, Phone: +44 151 231 2525, Fax: +44 151 231 2529

auxeticity of the materials [19]. But in the membrane or transition between plate and membrane behaviour, positive or negative Poisson's ratio theoretically would potentially have different effects under localised loading conditions [19-20]. It is essential to study the effect of Poisson's ratio on the material behaviour in both point loading and finite contact conditions (such in the case of a spherical indenter). Under these conditions which are different from the loading conditions of standard tests, the effect of material properties on the material behaviour is directly influence by the dimensions of the experimental samples as well as the loading conditions. A detailed understanding of these factors will help to establish the effects of the Poisson's ratio with a focus on the influence of auxeticity, which will help to further develop material testing methods and extend the use of auxetic materials in many relevant industrial fields.

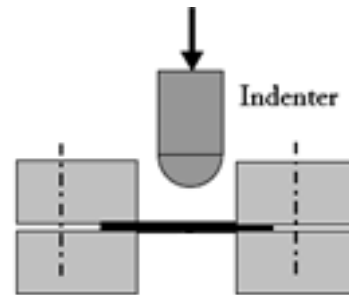
In this work, numerical models of a thin membrane under point loading and finite contact conditions with a spherical indenter have been developed. The FE model for the spherical indentation model is fully validated against experiment data of latex rubber samples (as a model material) of different thicknesses and sizes. The FE model simulating point loading of thin membranes is compared to analytical solutions for materials of different thicknesses and effects of the Poisson's ratio with different sample thickness and deflection depth is analysed. FE models with finite contact are developed to simulate thin membranes incorporating auxetic behaviour and their deformation mechanisms under an indentation bending test is studied. The effect of auxeticity on the P-h curves, deformation profile and contact is presented and discussed with reference to deformation mechanisms and potential use of auxeticity.

2 Experimental and FE models

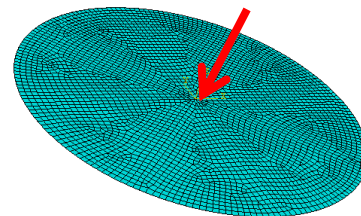
2.1 Experimental Fig. 1a shows schematically the setup of the indentation bending test. In the test, a spherical indenter is pressed onto a thin membrane supported by a circular frame which provides a fixed boundary condition. The diameter (designated as chamber size) and height of the supporting chamber is 30mm and 50mm, respectively. The radius of the indenter is 4mm. A rubber sheet with a thickness of 0.8 mm was made out of a latex resin by casting. The Young's modulus of the rubber sheet is 1.25MPa. The sample was made by mixing the latex coagulant and emulsion (ABL Resin & Glass, UK) at room temperature followed by degassing in a vacuum casting machine to remove entrained air, then pouring into an aluminum mold and cured at room temperature to avoid any residual pre-strain. The samples were characterised in uniaxial tensile tests and planar tests on a tensile test machine (Tinius Olsen Ltd (H50KS)), the data was used to validate the FE modeling results of the indentation bending tests. The indenter used is made of a stainless steel ball with a highly polished surface. The indentation system was mounted on a rigid supporting frame. The loading rate used in the test is 0.5mm/sec. A sensitive

load cell (model: LCMS-D12TC-5N) was attached to the moving head of the actuator to monitor the force during the test. The displacement of the indenter is monitored by a linear variable displacement transducer (LVDT) and controlled by a computer.

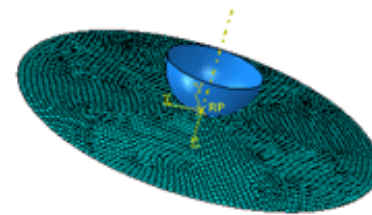
2.2 FE models



(a) Schematic to show the setup of a typical indentation bending test;



(b) FE model for for point loading of circular membrane.



(c) FE model for finite contact condition of circular membrane.

Figure 1 Setup of a typical indentation bending test (a) and FE model for point loading (b) and finite contact (c) of a thin membrane. The rim of the circular membrane is fixed at all degree of freedom.

The FE of the test is developed using the finite element program ABAQUS 6.11. Fig. 1 (b&c) shows the FE models developed to study the deformation of membranes under point loading (b) and finite contact condition (c). The membrane was modelled with shell elements (type S3 and S4R). There are in total ~15000 elements in the model with finer meshes over the region underneath the indenter in order to

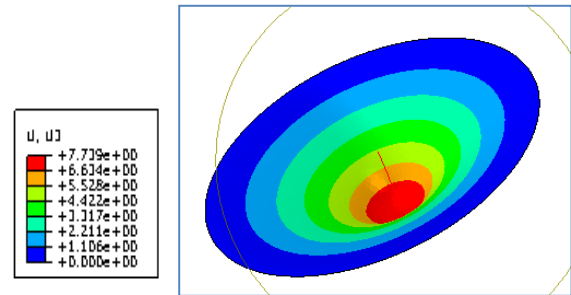
1 accurately establish the contact area. Both element types are
 2 general purpose conventional stress displacement shells
 3 with 3 or 4 nodes. These elements allow transverse shear
 4 deformation. The elements use thick shell theory as the shell
 5 thickness increases and become discrete Kirchhoff thin shell
 6 elements as the thickness decreases. The use of mixed types
 7 of elements effectively improved the efficiency of the FE
 8 model. The rim of the rubber sheet was fully fixed to represent
 9 the effect of the clamping rig. Preliminary work showed that
 10 the numerical results from this simplified (but more efficient)
 11 boundary condition were comparable to a solid model with full
 12 boundary conditions. A full 3D model also allows the evaluation
 13 of potential effects of misalignment etc. better than 2D models.
 14 The main work reported in this paper is based on a linear elastic
 15 law in which the properties were represented by Young's modulus
 16 (E) and the Poisson's ratio (ν). Linear elastic models have
 17 been used previously to describe rubber like membranes at relatively
 18 lower strain levels [1, 3]. In this work, the suitability of linear
 19 elastic modelling is also compared to several hyperelastic models
 20 to further validate the FE model and establish a displacement
 21 range, within which the linear elastic mode is valid. The use of
 22 linear elastic modelling allows effective evaluation of the effect
 23 of Poisson's ratio and auxeticity on the material behaviour in
 24 terms of force displacement data and deformation behaviours.

25
 26
 27
 28
 29 As shown in Fig.1 (b&c), two loading conditions have been
 30 investigated. One (Fig. 1b) is to apply a point load at the
 31 centre of the circular membrane; this is designed to compare the
 32 FE modelling results with analytical solutions. The other one
 33 (Fig. 1c) is a finite contact situation in which indenters of
 34 different sizes are simulated. In this case, contact has been
 35 defined between the indenter and specimen. Sensitivity tests
 36 have been performed to assess the influence of mesh size,
 37 boundary conditions, and frictional condition in order to ensure
 38 the FE model is accurate with an optimum requirement with
 39 regard to computational resources. A python program has been
 40 developed in which the material properties and sample thickness
 41 can be changed systematically.

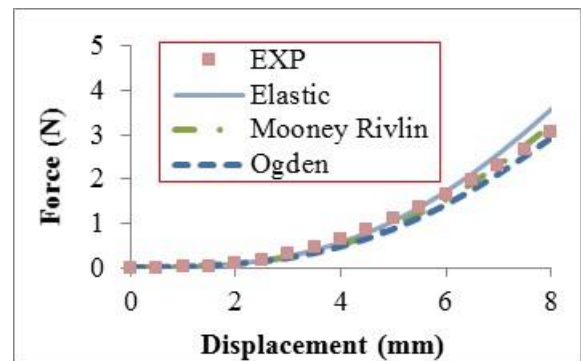
3 Results and discussion

42
 43
 44
 45
 46
 47 **3.1 Comparison between experimental data and FE modelling**
 48 Fig. 2 shows the displacement fields (a) and comparison between
 49 test data of the latex rubber sample and FE modelling with elastic
 50 properties (solid line) and hyperelastic properties (dashed line).
 51 Details of the Ogden and Mooney Rivlin strain energy functions
 52 could be found in the ABAQUS 6.11 Theory Manual. The linear
 53 elastic property is based on tensile tests and hyperelastic property
 54 is based on the combination of tensile and planar tests. The
 55 material test data is not shown to preserve clarity. The data in
 56 Fig. 2 clearly shows that the FE data with linear elastic properties

is in a good agreement with the testing data up to a displacement
 of 5mm. While the hyperelastic models can produce data up to
 much larger displacement. Given the current work is focused on
 investigating the effects of Poisson's ratio, the modelling is
 limited to the strain range where the linear elastic model is
 valid. Similar agreements could be found between FE and
 experimental data over a wide range of sample thickness and
 indenter sizes which confirms that the FE model is valid and
 accurate. This is essential to be able to predict the effects of
 Poisson's ratio and auxeticity.



(a) Typical deflection (U3: vertical displacement in mm) fields of membrane under indentation.



(b) Experimental force deflection data and FE results with linear elastic and hyperelastic material laws. ($E=1.25\text{MPa}$).

Figure 2 Comparison of experimental and numerical data with linear elastic and hyperelastic models to validate the FE model.

3.2 Deformation of a thin membrane under point loading conditions. Fig.3 compares the FE modelling results and analytical solution. The analytical solution (equation 1) is based on a modified Schwerin point loading condition with consideration of the influence of the Poisson's ratio [20].

$$\delta = f(\nu)a \left(\frac{P}{Eat} \right)^{\frac{1}{3}} \quad (1)$$

Where:

$$f(\nu) \approx 1.049 - 0.146\nu - 0.158\nu^2 \quad (2)$$

In equation (1), 'a' is the dimension of the chamber; ' δ ' is the indentation depth/deflection; 'P' is the force (N) and 't' is the sample thickness. The data presented in Fig. 3 are for membrane thickness of 0.1mm, $E=1.25\text{MPa}$ and Poisson's ratio of 0.495 and -0.495 (these value are used rather than 0.5 to improve the modelling efficiency). In both cases, the FE data and the analytical data show a good agreement.

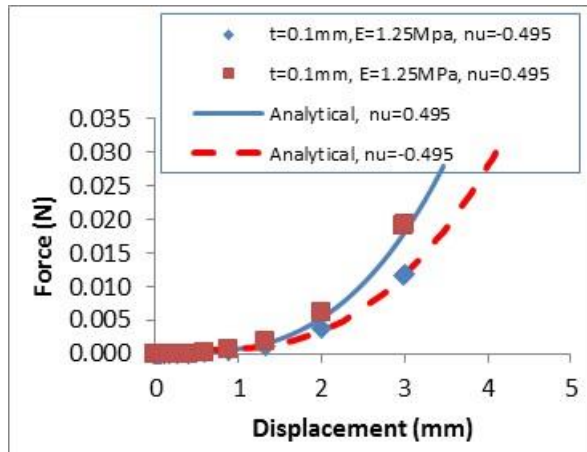
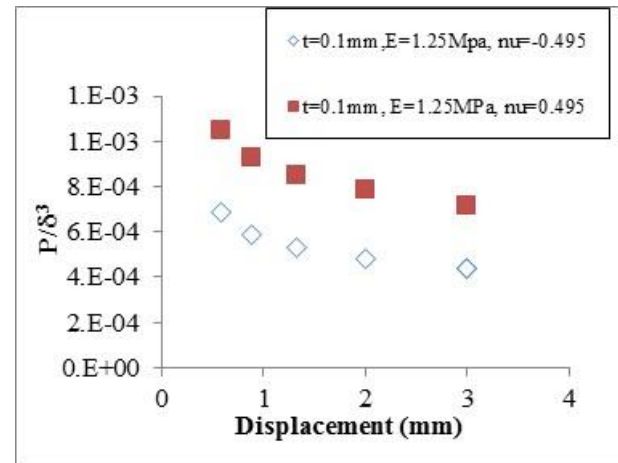
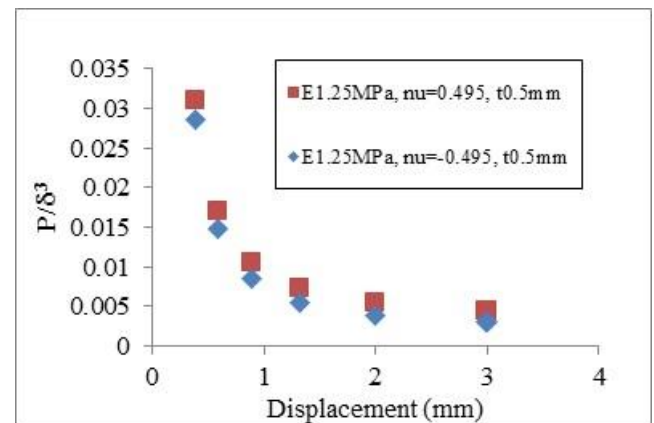


Figure 3 Comparison between FE and analytical solution for point loading condition of circular membrane with negative and positive poisson's ratio.

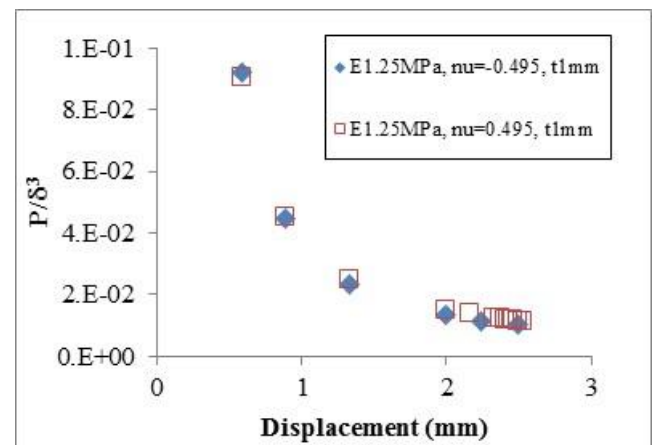
According to the analytical solution, P is related to δ^3 . Fig.4 plots (P/δ^3) vs. displacement. At lower displacement, P/δ^3 decreases with displacement following a similar trend between negative and positive Poisson's ratio, and then eventually reach to a stable value. With thin samples (a), there is a clear effect of auxeticity, (P/δ^3) is much lower with negative Poisson's ratio. As the thickness of the sample increase, the effect of negative Poisson's ratio become less significant, as shown in Fig 4b&c. In the case with a sample thickness of 1mm, the difference between positive and negative Poisson's ratio becomes much less significant.



(a) $t=0.1\text{mm}$



(b) $t=0.5\text{mm}$



(c) $t=1\text{mm}$

Figure 4 Variation of curvature parameter (P/δ^3) with positive and negative Poisson's ratio for samples of different thicknesses under point loading.

3.3 Effect of Poisson's ratio on the deformation of membranes under finite contact conditions.

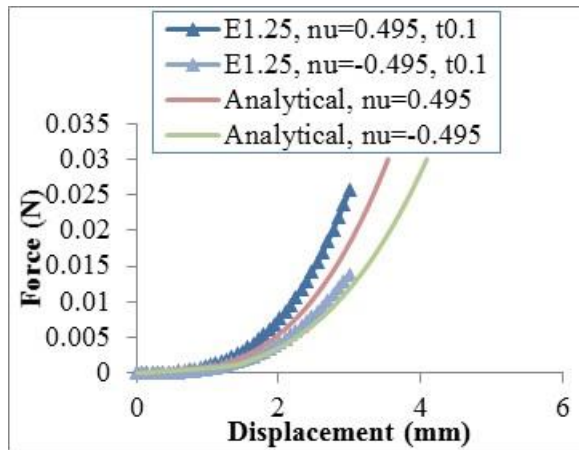
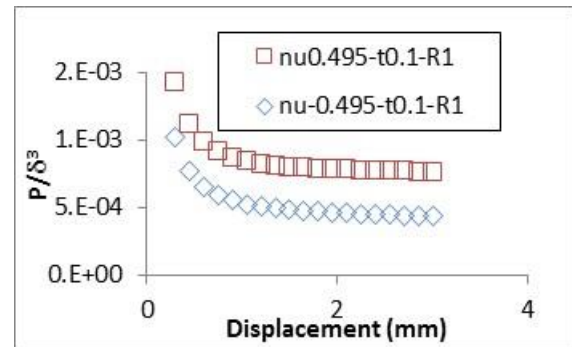
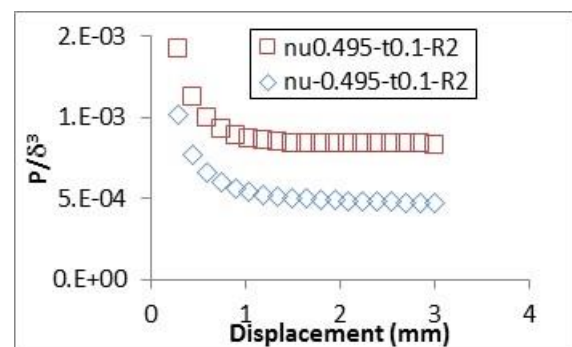


Figure 5 Force displacement curves for limit contact model. The solid and dash lines are data based on analytical solution for point loading (Eq.1).

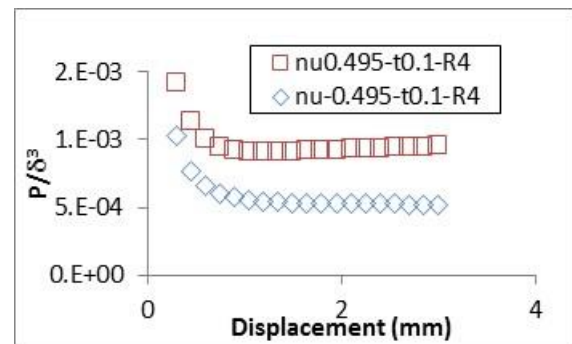
In the case of finite contact, an indenter is pressed onto the sample surface. Fig.5 shows typical force displacement data with an indenter size of R4mm. The data shows that the force displacement of a finite contact conditions is different from the analytical solution derived for point loading in particular at high indentation depths. Preliminary work also showed that only when the indenter size is smaller than 0.5mm, the result can be approximated by the analytical solution (results not shown). As shown in the data, the membrane with negative Poisson's ratio is weaker than the corresponding one with a positive Poisson's ratio. This is also observed for other E values. In other words, a material with a negative Poisson's ratio has better sensitivity to the load change. This could be a beneficial factor in situations such as sensors or some biological tissue such as bladder tissues. Fig. 6 plots P/δ^3 data for different indenter sizes. Results show that, in all cases, the deformation can be effectively represented/approximated by a cubic relationship, i.e. P/δ^3 , which could provide an effective way in material data comparisons. Comparing to the data metric for point loading conditions (Fig. 4), the P/δ^3 reached a stable constant zone at certain displacement ranges (in this case, after 1mm depth). This is probably due to the interaction between the membrane and the indenter. This could a very useful feature in representing the force displacement data. In the data for each indenter size, the P/δ^3 is lower for the membrane with a negative Poisson's ratio. Fig. 7 shows the P/δ^3 data for samples of different thicknesses. It clearly shows that the effect of auxeticity becomes less significant for thicker samples.



(a) R=1mm.



(b)R=2mm.



(c) R=4mm.

Figure 6 Curvature Parameter (P/δ^3) vs. depth for different indenter sizes (R1, 2, and 4mm, sample thickness=0.1mm).

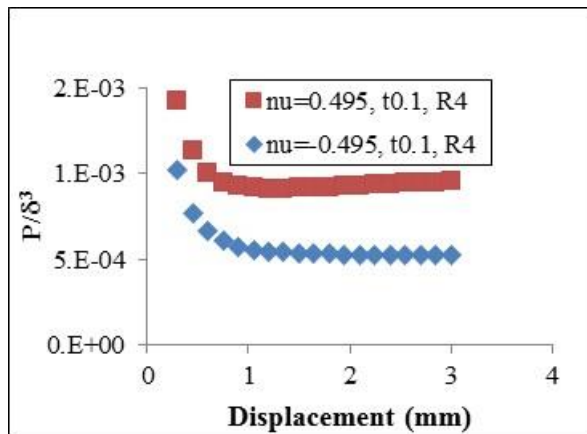
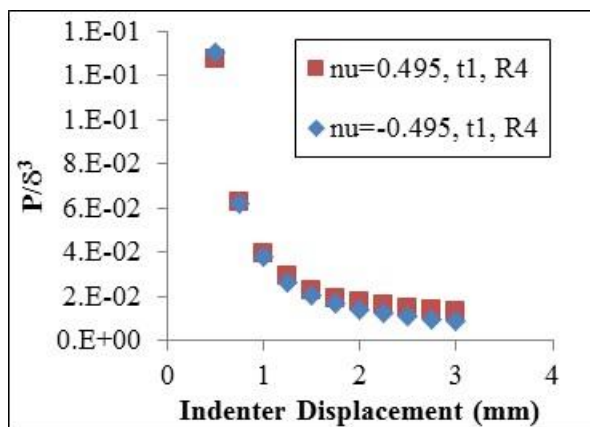
(a) $t=0.1\text{mm}$.(b) $t=1\text{mm}$.

Figure 7 Effect of auxeticity on the P/δ^3 for samples of different thickness.

These results clearly show that auxeticity has direct influences on the force displacement relationship. The detailed deformation is analysed to establish the effect of auxeticity on the displacement profile for both the vertical ($U3$) and radial ($U1$) direction. Different from standard material tests, the displacement profile is an important feature for thin membrane tests. The profile may provide means to represent the deformation of the materials, which has been explored by several researchers [1, 4]. It is important to analyse the potential effects of auxeticity on the displacement profile and contact conditions. Fig.8 plots a typical profile of vertical deflection ($U3$) with positive and negative Poisson's ratio. In the figure, the x-axis used is the distance from the centre point normalised by the radius of the chamber (15mm). (0 represents the central point, 1 represents the position of the edge). For thin samples, the displacement profile between the positive and negative Poisson's ratio is slightly different (Fig. 8a). The general displacement profile

is comparable in the central part and near the clamp edge, probably due to restraint from the indenter and the edge effects. But with thicker specimen, there is less significant difference in the displacement profile between positive and negative Poisson's ratio. This is probably associated with the transition to the plate deformation domain.

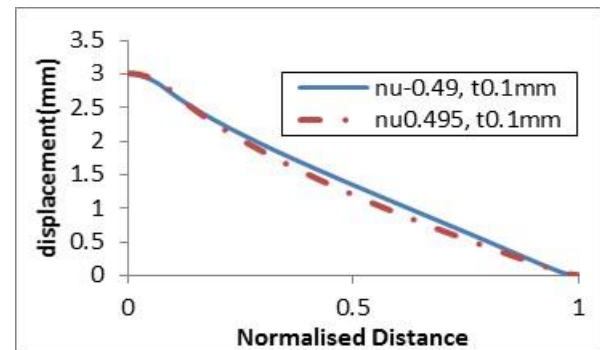
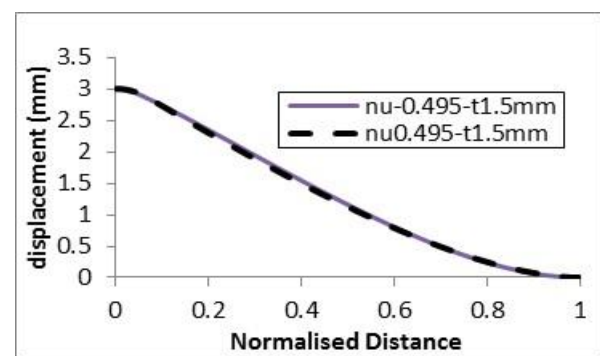
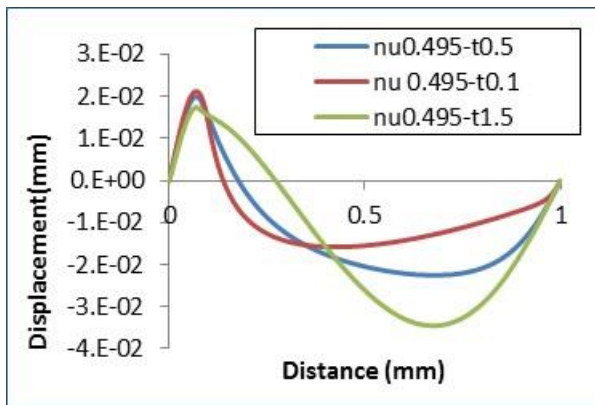
(a) Vertical displacement ($U3$), $t=0.1\text{mm}$, R4.(b) Vertical displacement ($U3$), $t=1.5\text{mm}$, R4.

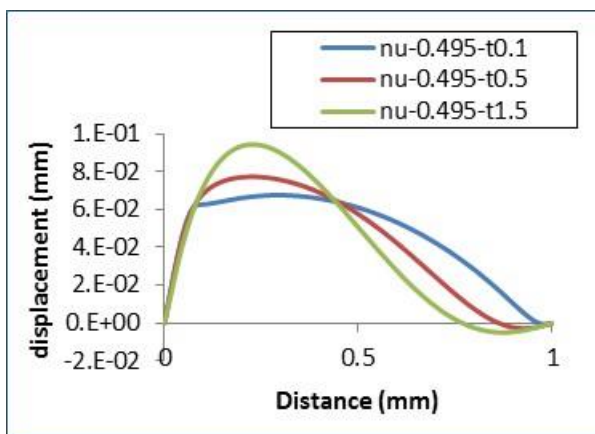
Figure 8 Effect of auxeticity on the displacement (Vertical displacement, $U3$) profile with different sample thickness.

Fig. 9 (a & b) compares the profiles of radial displacement ($U1$) for samples with different thicknesses at an indentation depth of 3mm. In all cases, the auxeticity showed a clear influence on the profile. In general, the displacement values are very low, but there is a clear difference between these two sets of data. The data suggests that a negative Poisson ratio results in a positive radial displacement (Fig. 9b) as comparison to a predominantly negative radial displacement in the case of a positive Poisson's ratio (Fig. 9a). With finite contact problems, the contact area is another important character. This could be estimated by plotting the contact pressure from the FE model. Fig. 10 shows the contact pressure for samples of different thicknesses. In both cases, the contact area for the negative Poisson's ratio one is smaller than the one with positive Poisson's ratio, with more significant difference for the thin samples. This is in a

reasonable agreement with the data on the deformation profiles and force displacement data.

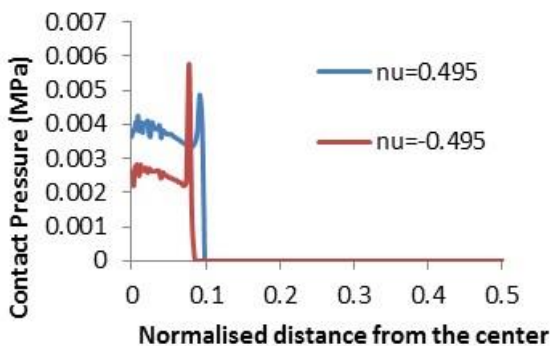


(a)

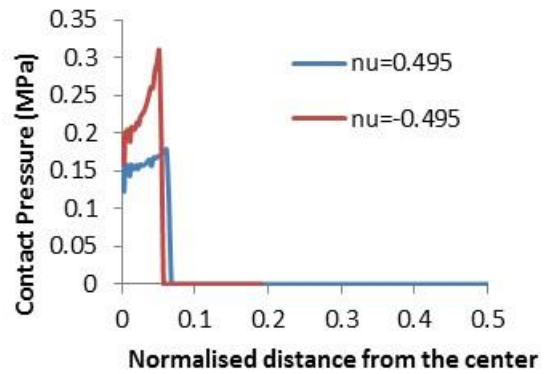


(b)

Figure 9 Radial displacement (U1) profile with different sample thicknesses.



(a) $t=0.1\text{mm}$, R4.



(b) $t=1.5\text{mm}$, R4.

Figure 10 Effect of Poisson's ratio on the contact pressure showing the effect of auxeticity on the contact area.

The effect of the auxeticity on the contact and the deformation of thin plate is a complex process, as the deformation of the region in contact with the indenter and the remaining region of the membrane could be through different deformation regimes [20]. The contact pressure is affected by many factors such as the friction, thinning of the samples and chamber size, which require a systematic further investigation. The change of the contact area observed is in reasonable agreement with the effects of negative Poisson's ratios. In general, for an auxetic membrane, there is a tendency for circumferential strain to be positive causing expanded radius. An expanded radius, in the case of finite contact, would naturally give a decreased contact area. This in turn may affect the overall indentation resistance. Further work is required to investigate if these changes of the contact area have partially contributed to the relative lower force for materials with a negative Poisson's ratio.

4 Conclusions

In this work, the deformation of circular elastic membranes with a clamped edge under point loading and finite contact conditions is systematically studied incorporating auxeticity behaviour. The effect of Poisson's ratio on the deformation of the material is established. The feasibility and limitation of an analytical solution is assessed. The work shows that the P/δ^3 relationship is applicable to describe the force displacement data over the membrane domain for both point loading and finite contact conditions. It is shown that negative Poisson's ratio has direct influence on the membrane deformation domain; the force is relatively lower, which could be beneficial as the material will be more sensitive to load change. The deflection profile is slightly different between positive and negative Poisson's ratio, while the contact area for negative Poisson's ratio is relatively smaller. This work has highlighted some important characteristics of membranes with negative Poisson's ratio, further work is required to quantify these effects with

consideration of relative dimensions between sample thickness and chamber size.

References

- [1] B.F. Ju, Y. Ju, M. Saka, K. Liu, K. Wan, A systematic method for characterizing the elastic properties and adhesion of a thin polymer membrane, *Int. J. of Mechanical Sciences* 47 (2005) 319–332.
- [2] P. Egan, M.P. Whelan, F. Lakestani and M. J. Connelly, Small punch test: An approach to solve the inverse problem by deformation shape and finite element optimization, *Computational Materials Science* 40 (2007) 33–39.
- [3] O.N. Scott, M.R. Begley, U. Komaragiri and T.J. Mackin, Indentation of freestanding circular elastomer films using spherical indenters, *Acta Materialia* 52 (2004) 4877–4885.
- [4] A.P.S. Selvadurai, Deflections of a rubber membrane, *J. of the Mechanics and Physics of Solids* 54 (2006) 1093–1119.
- [5] M. Ahearne, K.K. Liu, A.J. El Haj, K.Y. Then, S. Rauz, Y. Yang, Online monitoring of the mechanical behaviour of collagen hydrogels: influence of corneal fibroblasts on elastic modulus. *Tissue Eng Part C Methods*, vol. 16(2) (2010) 319–327.
- [6] R. Perlrine, R. Kornbluh, J. Joseph, R. Heydt, Q. Pei and S. Chiba, High-field deformation of elastomeric dielectrics for actuators, *Mater Sci Eng C* 11(2000) 89–100.
- [7] K.K. Liu, B.B. Ju, A novel technique for mechanical characterization of thin elastomeric membrane, *J Phys D: Appl Phys* 34 (2001)91–94.
- [8] M.L. Oyen, R.E. Cook, S.E. Calvin, Failure of Human Fetal Membrane Tissues, *J Mater Sci: Mater Med* 15 (2004) 651–8.
- [9] D.M. Haughton, *Nonlinear Elasticity: Theory and Applications* (Fu, Y.B., Ogden, R.W. (Eds.), Cambridge University Press) 283 (2001) 233–267.
- [10] D.J. Steigmann, Puncturing a thin elastic sheet, *Int. J. Non-Linear Mech.* 40 (2005) 255–270.
- [11] K. E. Evans and A. Alderson, Auxetic Materials: Functional Materials and Structures from Lateral Thinking!, *Advanced Materials*, 12(9) (2000) 617–628.
- [12] M. Sanami, N. Ravirala, K. Alderson, A. Alderson, Auxetic Materials for Sports Applications, *Procedia Engineering*, 72 (2014) 453–458.
- [13] K. Alderson, A. Alderson, J.N. Grima, K. W. Wojciechowski, Auxetic Materials and Related Systems, *physica status solidi (b)*, 251(2) (2014) 263–266.
- [14] Z. Ge and H. Hu, Deformation behaviors of three-dimensional auxetic spacer fabrics, *Journal of the Textile Institute*, 106 (2015)101–109.
- [15] A.A. Pozniak and K.W. Wojciechowski, Poisson's ratio of rectangular anti-chiral structures with size dispersion of circular nodes, *Physica Status Solidi B*, 251 (2014)367–374.
- [16] T.C. Lim, *Auxetic Materials and Structures*. Springer, Singapore (2015).
- [17] J. Sun, H. Gao, F. Scarpa, C. Lira, Y. Liu and J. Leng, Active inflatable auxetic honeycomb structural concept for morphing wingtips, *Smart Materials and Structures* 23 (2014), 125023.
- [18] I. Shufrin, E. Pasternak, and A. V. Dyskin, Hybrid materials with negative Poisson's ratio inclusions, *Int. J. Eng. Sci.* 89 (2015)100–120.
- [19] S. Timoshenko and S. Woinowski-Krieger, in *Theory of Plates and Shells* (McGraw-Hill, New York, 1987)
- [20] U. Komaragiri, M. R. Begley and J. G. Simmonds, The Mechanical Response of Freestanding Circular Elastic Films Under Point and Pressure Loads, *J. Appl. Mech.* 72(2) (2005) 203–212.